Dawn E.W. Livingstone, Pascal Barat, Emma M. Di Rollo, Georgina A. Rees, Benjamin A. Weldin, Eva A. Rog-Zielinska, David P. MacFarlane, Brian R. Walker, and Ruth Andrew

5α-Reductase Type 1 Deficiency or Inhibition Predisposes to Insulin Resistance, Hepatic Steatosis, and Liver Fibrosis in Rodents

Diabetes 2015;64:447–458 | DOI: 10.2337/db14-0249

5α-Reductase type 1 (5αR1) catalyses A-ring reduction of androgens and glucocorticoids in liver, potentially influencing hepatic manifestations of the metabolic syndrome. Male mice, homozygous for a disrupted 5αR1 allele (5αR1 knockout [KO] mice), were studied after metabolic (high-fat diet) and fibrotic (carbon tetrachloride [CCl_4]) challenge. The effect of the 5α-reductase inhibitor finasteride on metabolism was investigated in male obese Zucker rats. While eating a high-fat diet, male 5αR1-KO mice demonstrated greater mean weight gain (21.6 ± 1.4 vs 16.2 ± 2.4 g), hyperinsulinemia (insulin area under the curve during glucose tolerance test 609 ± 103 vs. 313 ± 66 ng · mL^{-1} · min), and hepatic steatosis (liver triglycerides 136.1 ± 17.0 vs. 89.3 ± 12.1 μmol · g^{-1}). mRNA transcript profiles in liver were consistent with decreased fatty acid β-oxidation and increased triglyceride storage. 5αR1-KO male mice were more susceptible to fibrosis after CCl_4 administration (37% increase in collagen staining). The nonselective 5α-reductase inhibitor finasteride induced hyperinsulinemia and hepatic steatosis (10.6 ± 1.2 vs. 7.0 ± 1.0 μmol · g^{-1}) in obese male Zucker rats, both intact and castrated. 5αR1 deficiency induces insulin resistance and hepatic steatosis, consistent with the intrahepatic accumulation of glucocorticoids, and predisposes to hepatic fibrosis. Hepatic steatosis is independent of androgens in rats. Variations in 5αR1 activity in obesity and with nonselective 5α-reductase inhibition in men with prostate disease may have important consequences for the onset and progression of metabolic liver disease.

Steroid hormone signaling has a potent influence on fuel metabolism and body fat distribution, and altered signaling has been implicated in many aspects of metabolic syndrome, including liver fat accumulation in nonalcoholic fatty liver disease. Steroid receptor activation is modulated not only by circulating steroid concentrations but also by prereceptor metabolism within target tissues. For example, receptor activation is amplified by aromatase (for estrogen receptors) and 11β-hydroxysteroid dehydrogenase type 1 (for glucocorticoid receptors). These enzymes alter intracellular steroid concentrations independently of circulating concentrations, thereby influencing metabolic physiology and disease (1–3), and have provided therapeutic targets in patients with breast cancer and type 2 diabetes, respectively.

The isozymes of 5α-reductase (5αR) also regulate cellular steroid levels (4,5). 5αR type 2 (5αR2) is highly expressed in the prostate, where it amplifies androgen action by converting testosterone into the more potent androgen 5α-dihydrotestosterone, and is inhibited by finasteride in the treatment of prostate disease. 5αR type 1 (5αR1) is expressed in the human male reproductive tract but also highly in the liver (5), and at lower levels in adipose tissue (6,7) and skeletal muscle (8),

University/British Heart Foundation Centre for Cardiovascular Science, Queen's Medical Research Institute, University of Edinburgh, Edinburgh, U.K.

Corresponding author: Dawn E.W. Livingstone, dawn.livingstone@ed.ac.uk.

Received 13 February 2014 and accepted 29 August 2014.

This article contains Supplementary Data online at http://diabetes.diabetesjournals.org/lookup/suppl/doi:10.2337/db14-0249/-/DC1.

P.B. is currently affiliated with the Université de Bordeaux, Nutrition et Neurobiologie Intégrée, UMR 1286, Bordeaux, France.

where it metabolizes a variety of pregnene steroids, including androgens and glucocorticoids (9); and is inhibited by the nonselective inhibitor of 5αRs, dutasteride (10). 5α-Reduction contributes substantially to the clearance of glucocorticoids: corticosterone in rodents, and cortisol in humans. Mice deficient in 5αR1 have an eightfold slower clearance of corticosterone (11), and in humans, 5α-reduced glucocorticoids comprise approximately one-third to one-half of urinary cortisol metabolites (12).

Increased excretion of 5α-reduced steroids has been observed in obesity, polycystic ovarian syndrome, and nonalcoholic fatty liver disease (12–17), while decreased excretion occurs in critical illness (18). The associated changes in cortisol clearance rate are thought to influence the hypothalamic-pituitary-adrenal axis in these conditions. We have previously demonstrated that mice deficient in 5αR1 accumulate excess glucocorticoid in liver and adipose (11), which may have direct consequences for glucocorticoid receptor activation. A recent report (19) shows that mice lacking 5αR1 are more prone to hepatic steatosis, but with no apparent differences in body fat distribution or insulin sensitivity and with protection from hepatocellular carcinoma; the mechanisms remain unclear, in particular the independent roles of glucocorticoid and androgen metabolism. However, they are important to elucidate as the finding that deficiency in 5αR1 adversely affects metabolism translates into human health. We have recently demonstrated that dual pharmacological inhibition of 5αR1 and 5αR2 (but not 5αR2 alone) adversely affects metabolism, causing increased adiposity and insulin resistance (20).

Here we hypothesize that 5αR deficiency or inhibition in the liver leads to local accumulation of glucocorticoids, enhanced glucocorticoid receptor activation and consequent insulin resistance, hepatic steatosis, and susceptibility to nonalcoholic fatty liver disease. In mice and rats, only 5αR1 is expressed in the liver, unlike humans in whom both isozymes of 5αRs are expressed (4). In rats, finasteride is a nonselective inhibitor of both 5αR1 as well as 5αR2 (21). We therefore tested our hypothesis using mice with targeted deletion of 5αR1 (22,23) and after pharmacological inhibition with finasteride in rats.

RESEARCH DESIGN AND METHODS

Chemicals were from Sigma (Poole, U.K.) unless otherwise stated. Solvents were glass distilled high-performance liquid chromatography grade (Fisher Scientific, Loughborough, U.K.). Steroids were from Steraloids (Newport, RI).

Embryos (C57BL6/SvEv/129) with targeted disruption of 5αR1 (22,23) (The Jackson Laboratory, Bar Harbor, ME) were rederived, and heterozygote offspring were crossed to generate homozygote male "wild-type" (WT) and "knockout" (KO) mice (5αR1-KO mice). Male obese Zucker rats and their lean controls were from Harlan Olac (Bicester, U.K.). Animals were studied under U.K. Home Office license with free access to drinking water and either standard chow (7.4% fat, 4% sucrose; RM1; Special Diet Services, Witham, U.K.) or experimental diets. Animals were killed (0800–1100 h) by decapitation; trunk blood was collected; and tissues were dissected, wet weighed, and either snap frozen or fixed in formalin.

Investigations of Metabolic Function in 5αR1-Deficient Mice

Weight gain was monitored in male WT and 5αR1-KO mice maintained on chow. Intraperitoneal glucose (2 mg/g) tolerance tests (GTTs) were performed after a 6 h fast with a tail-tip bleed (at 0, 15, 30, 60, and 90 min).

Responses to High-Fat Feeding

For high-fat feeding, male WT and 5αR1-KO mice aged ~5 months were housed individually (n = 7–9/group), with free access to either a Western style high-fat, high-sucrose diet (58% kcal fat, 13% kcal sucrose) or a control diet (10.5% kcal fat, 0% kcal_sucrose; Research Diets Inc, New Brunswick, NJ). Body weight and food consumption were recorded weekly. GTTs were performed after 1, 3, and 6 months of feeding on a diet, as described above. Mice were allowed to recover for 1 week before being culled.

Susceptibility to Liver Injury

WT and 5αR1-KO male mice (~5 m) were treated by intraperitoneal injection with 0.3 μL/g carbon tetrachloride (CCl_4) in olive oil (n = 8/group) or vehicle (n = 4/group) twice weekly for 6 weeks (24). Body weight was recorded weekly, and mice were culled 48 h after the last injection with CCl_4.

Metabolic Effects of Pharmacological Inhibition of 5αR

Zucker rats (n = 10–15/group, 6 weeks of age) were treated with the 5αR inhibitor finasteride (0.35 mg/kg/d) or vehicle (5% ethanol; 1 mL/kg/d) by daily gavage. Finasteride inhibits both isozymes of 5αR in rats (21,25). After 2 weeks, the results of an oral GTT were assessed at 0, 30, and 120 min after glucose bolus administration (26). After a further week of treatment, rats were killed. Livers were snap frozen and processed for transcript analysis. The experiment was repeated in a second cohort of obese rats who had undergone either bilateral gonadectomy or sham surgery (6) 4 weeks prior to commencement of finasteride or vehicle treatment.

Laboratory Analyses

Plasma Biochemistry

Corticosterone was measured by radioimmunoassay (27), insulin by ELISA (Crystal Chem, Downers Grove, IL), glucose by the hexokinase method (Thermo Electron, Melbourne, Victoria, Australia), adipokines and apolipoproteins (apos) by Lincoplex immunoassays (Dundee, U.K.), and triglycerides and cholesterol (MICROgenics, Passau, Germany) and nonesterified fatty acids (NEFAs) (Zen-Bio) spectrophotometrically. Testosterone and finasteride were quantified in rat plasma (1 mL) as described previously (20) but were adapted for larger volume (1 mL) by use of Oasis HLB cartridges (60 cm^3; Waters, Elstree, U.K.).

Tissue Biochemistry

To measure triglycerides, 50–100 mg liver was mechanically homogenized in propan-2-ol (20 vol for mice on a high-fat diet; 10 vol for mice on a normal-fat diet and rats) and assayed spectrophotometrically (28).

Quantification of mRNAs by Real-Time Quantitative PCR

Total RNA was extracted using the Qiagen RNeasy system, and 500 ng was reverse transcribed into cDNA with random primers using the QuantiTect DNase/reverse transcription kit. cDNA (equivalent to 1 ng total RNA) was incubated in triplicate with gene-specific primers and fluorescent probes (Supplementary Table 1) (Universal Probe Library, Roche Diagnostics, Burges Hill, U.K.; or Applied Biosystems, Warrington, U.K.) in 1× Roche LightCycler 480 Probes mastermix. Quantitative PCR was carried out using a Roche LightCycler 480. A standard curve was constructed for each primer probe set using a serial dilution of cDNA pooled from all samples. Results were corrected for the arithmetic mean of abundance of reference genes (for high-fat experiment: *Ppia*, *Rn18s*, and *Tbp*; for CCl_4 experiment: *Actb* and *Ppia*; for rat experiment: *Ppia* and *Rn18S*), which did not differ between groups.

Quantitation of Hepatic Fibrosis

Fixed livers were sectioned (5 μm) and stained with hematoxylin-eosin or picrosirius red. Sections were examined by light microscopy (×10 magnification; Axio Scope microscope; Zeiss) and photographed using a CoolSNAP camera (Photometrics). Picrosirius red stain was quantified by counting the number of red pixels in 20 randomly selected fields of view from each section, using Adobe Photoshop version 5.0 software. Data are presented as the mean number of red pixels per field of view, which is representative of the amount of collagen stained.

Transcript Profile of 5αR1 and 5αR2 in Metabolic Tissues

The expression of 5αR1 and 5αR2 mRNAs was assessed in liver; subcutaneous adipose tissue and skeletal muscle from WT mice and rats; and prostate from rats as positive control for 5αR2. cDNA (10 ng; prepared as described above) was subjected to PCR using the Qiagen HotStarTaq Plus system (Qiagen, Crawley, U.K.), and products were electrophoresed on a 1.2% agarose gel in 0.5× Tris-borate-EDTA buffer. Primers were mouse 5αR1 tttgctcttcctttgggcta and ctgccatcaattccttggat, and 5αR2 aacacagcgagagtgtgtcg and cgcgcaataaaccaggtaat; and rat 5αR1 tttgctcttcctttgggcta and ccaaacagggtctccctaca, and 5αR2 gttgccttcctttgtggtgt and tgattcccatccccagaata.

Statistical Analysis

Data are reported as the mean ± SEM. Statistical analysis was performed using Statistica software (StatSoft). Groups were compared by Student *t* tests, two-way or repeated-measures ANOVA, with Fisher post hoc tests, with differences of $P < 0.05$ accepted as statistically significant. Areas under the curve were calculated using Kinetica software (Thermo Electron Corp., Hemel Hempstead, U.K.).

RESULTS

Transcript Profile of 5αR1 and 5αR2 in Metabolic Tissues

In the mouse (Fig. 1*A*), 5αR1 was expressed in liver and adipose tissue, and in skeletal muscle to a lesser degree. Transcript for 5αR2 was detectable only in liver and adipose tissue. In the rat (Fig. 1*B*), 5αR1 mRNA was again expressed in liver and skeletal muscle, and less so in

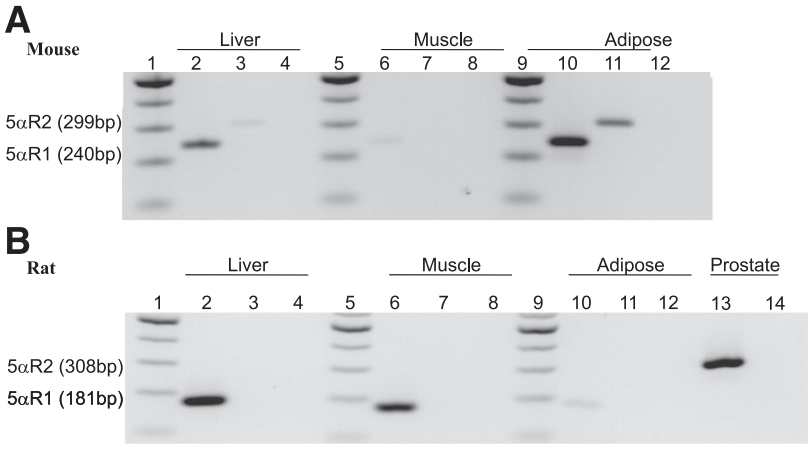

Figure 1—Transcript profile of 5αR1 and 5αR2 in metabolic tissues of mice and rats. *A*: In mice, 5αR1 (240 BP) was detected in liver, skeletal muscle, and adipose tissue, whereas 5αR2 (299 BP) was only detectable in liver and adipose tissue. *B*: In the rat, 5αR1 (181 BP) was detected in liver, skeletal muscle, and adipose tissue, whereas 5αR2 (308 BP) was only detectable in the prostate positive control. *A* and *B*: Lanes 1, 5, and 9, 100 BP ladder; lane 2, liver 5αR1; lane 3, liver 5αR2; lane 4, liver negative control; lane 6, muscle 5αR1; lane 7, muscle 5αR2; lane 8, muscle negative control; lane 10, adipose 5αR1; lane 11, adipose 5αR2; lane 12, adipose negative control. *B*: Lane 13, prostate 5αR2; lane 14, prostate negative control.

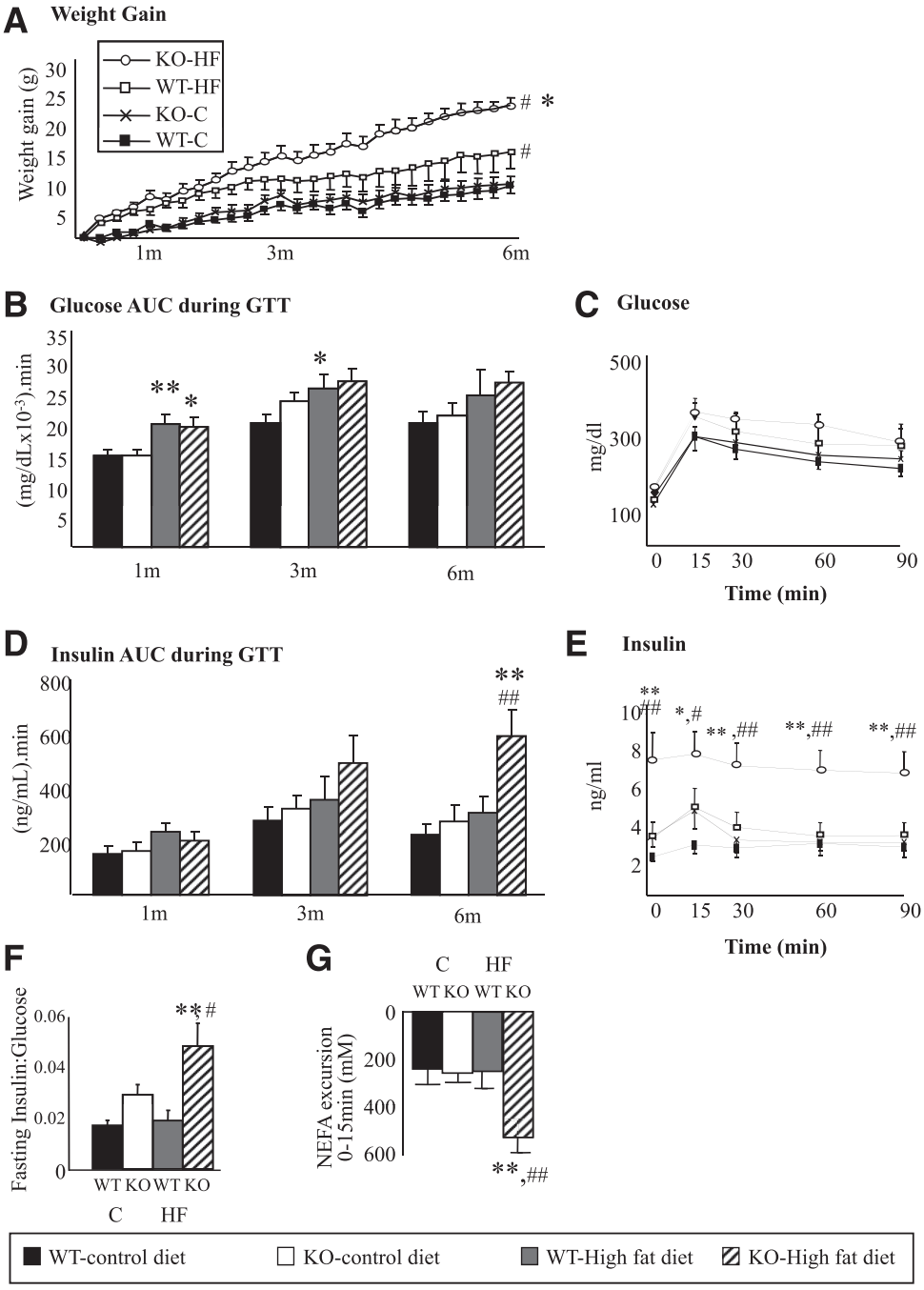

Figure 2—Metabolic phenotype in male 5αR1-KO and WT mice. 5αR1-KO mice and their littermate controls (WT) were fed standard chow until age 5 months, after which they were given experimental diets containing high fat or a matched control diet for 6 months. Differences in weight gain were not observed between genotypes on a chow diet (*A*), but KO mice gained more weight than WT mice on a high-fat diet (*B*). The AUC of glucose during an intraperitoneal GTT did not differ from that of WT mice with age or in response to a high-fat diet. *C*: Time courses of plasma glucose during GTT after 6 months on a high-fat diet. *D*: The AUC of insulin during the GTT was significantly greater in KO mice upon consumption of a high-fat diet for 6 months. *E*: Time course of plasma insulin responses during the GTT after 6 months of eating a high-fat diet. *F*: Fasting ratios of insulin to glucose were greater in KO mice compared with WT mice after a 6-month high-fat diet. *G*: Suppression of NEFAs during the first 15 min of the GTT (i.e., after the glucose bolus at time 0). Black bars denote WT mice and open bars denote KO mice eating a control diet; gray bars denote WT and striped bars denote KO mice eating a high-fat diet. Data are reported as the mean ± SEM, compared by Student *t* test or two-way ANOVA followed by post hoc testing with Fisher LSD test, if appropriate. **P* < 0.05, ***P* < 0.01 for difference between genotypes within a diet; #*P* < 0.05, ##*P* < 0.01 for effect of diet within genotype. C, control diet; HF, high-fat diet; NS, not significant. *n* = 7–9/group.

adipose tissue, but the transcript for 5αR2 was detectable only in the prostate. The abundance of mRNA for 5αR1 in the liver of WT mice was not changed in response to a high-fat diet (Supplementary Table 3).

5αR1 Deficiency Increases Susceptibility to Metabolic Dysfunction on High-Fat Feeding

5αR1-KO mice eating normal chow were not different in weight and had only minor differences in metabolic phenotype from WT mice before 5 months of age (Supplementary Table 2). Glucose intolerance was detected at 3 months of age, and a trend to hyperinsulinemia during GTT was detected at 5 months, but there was no difference in body fat.

While eating a high-fat diet, however, 5αR1-KO mice had increased susceptibility to weight gain (Fig. 2*A* and Supplementary Fig. 1), hyperinsulinemia (fasting and during GTT; Table 1 and Fig. 2*D* and *E*), fasting hyperglycemia (Table 1 and Fig. 2*C*), increased ratios of insulin to glucose (Fig. 2*G*), and liver fat accumulation (Fig. 3*C*). The excess weight gain was distributed among several organs, including liver and adipose depots (Table 1). Changes in plasma lipid and adipokine profiles with high-fat feeding differed only marginally from those of WT mice (Table 1). Suppression of lipolysis (measured by NEFA suppression in the first 15 min of the GTT) was enhanced in 5αR1-KO mice (Fig. 2*H*).

In the liver, the induction of gene transcripts encoding enzymes involved in fatty acid β-oxidation (*Cpt1a* and its transcriptional regulator *Pparα*) and gluconeogenesis (*Pepck* by eating a high-fat diet was impaired in 5αR1-KO mice, while transcripts of genes favoring triglyceride esterification (*Dgat2* and *Gpam*) and cholesterol synthesis and excretion (*Hmgcr* and *Apoa1*) were disproportionately increased (Fig. 3*D* and Supplementary Table 3*A*). In subcutaneous adipose tissue, *Ucp2*, *Scd*, and *Dgat1* were upregulated in response to high-fat feeding in 5αR1-KO mice compared with control mice (Fig. 3*E* and Supplementary Table 3*B*). In mesenteric adipose tissue, *Dgat2* was upregulated and *Cpt1* was not induced in high fat–fed 5αR1-KO mice (Fig. 3*F* and Supplementary Table 3*C*).

5αRI-KO Mice Are More Susceptible to Liver Fibrosis

There was no effect of CCl_4 challenge on body weight in either genotype (two-way ANOVA: $P = 0.4$ for treatment and $P = 0.6$ for genotype) or on liver weight (Fig. 4*A*). 5αR1-KO mice showed greater hepatic fibrosis than WT mice, which was indicated by increased picrosirius red staining for collagen (Fig. 4*B*), including evidence of bridging fibrosis (Fig. 5*D*). There was no difference between 5αR1-KO and WT mice in the induction of gene transcripts for inflammatory markers of hepatic stellate cell activation, proteases involved in collagen breakdown, or the majority of transcripts involved in collagen assembly and stability (Fig. 4*E* and *F* and Supplementary Table 4). However, compared with WT mice, 5αR1-KO mice had attenuated induction of *Leprel2* and *Loxl4*, enzymes involved in collagen assembly and cross-linking, and an exaggerated induction of the protease inhibitor *Timp1* (Fig. 4*E*). Fibrosis was associated with greater lipid depletion within the liver of 5αR1-KO mice (Fig. 4*C*), with increased plasma triglyceride concentration (Fig. 4*D*), and a transcript profile supportive of reduced lipid turnover (Fig. 4*G*), both by suppressed

Table 1—Indices of metabolism in 5αR1-KO mice vs. WT controls

	WT		5αR1-KO	
	Control	High fat	Control	High fat
Weight at cull (g)	41.0 ± 1.73	46.5 ± 2.7*	41.7 ± 1.4	54.1 ± 1.3*†
Fasting plasma glucose (mg/dL)	128 ± 8.7	149 ± 10.4	107 ± 9.1	142 ± 6.2*
Fasting plasma insulin (ng/mL)	3.16 ± 0.24	3.01 ± 0.88	2.03 ± 0.58	7.14 ± 1.4*†
Omental adipose weight (mg)	42 ± 4	57 ± 6	32 ± 3	57 ± 8*
Gonadal adipose weight (mg)	1,295 ± 143	2,273 ± 25*	1,231 ± 12	2,374 ± 219*
SubQ adipose weight (mg)	829 ± 95	1,585 ± 202*	894 ± 111	1,860 ± 193*
Quadriceps weight (mg)	209 ± 16	178 ± 12	211 ± 11	206 ± 9
Total adipose (mg)	3,634 ± 316	5,351 ± 319*	3,590 ± 320	6,793 ± 220*†
Plasma cholesterol (mmol/L)	1.98 ± 0.18	3.11 ± 0.39*	2.11 ± 0.19	3.71 ± 0.38*
Plasma triglycerides (mmol/L)	1.60 ± 0.19	2.07 ± 0.26	1.37 ± 0.07	1.62 ± 0.17
Plasma apoA1 (mg/mL)	1.01 ± 0.08	1.18 ± 0.22	1.11 ± 0.13	1.78 ± 0.23*†
Plasma apoE (μg/mL)	1.15 ± 0.16	1.81 ± 0.11*	1.15 ± 0.10	1.62 ± 0.11*
Plasma leptin (ng/mL)	6.7 ± 1.1	11.9 ± 1.4*	9.0 ± 1.8	9.9 ± 1.4
Plasma adiponectin (μg/mL)	19.3 ± 2.8	14.8 ± 0.9	17.5 ± 1.8	13.1 ± 0.9
Plasma resistin (ng/mL)	0.89 ± 0.07	1.73 ± 0.13	1.02 ± 0.13	1.08 ± 0.12†

Data are the mean ± SEM, compared by two-way ANOVA with Fisher post hoc tests. SubQ, subcutaneous. *$P < 0.05$ for effect of diet within genotype. †$P < 0.05$ for difference between genotypes within diet.

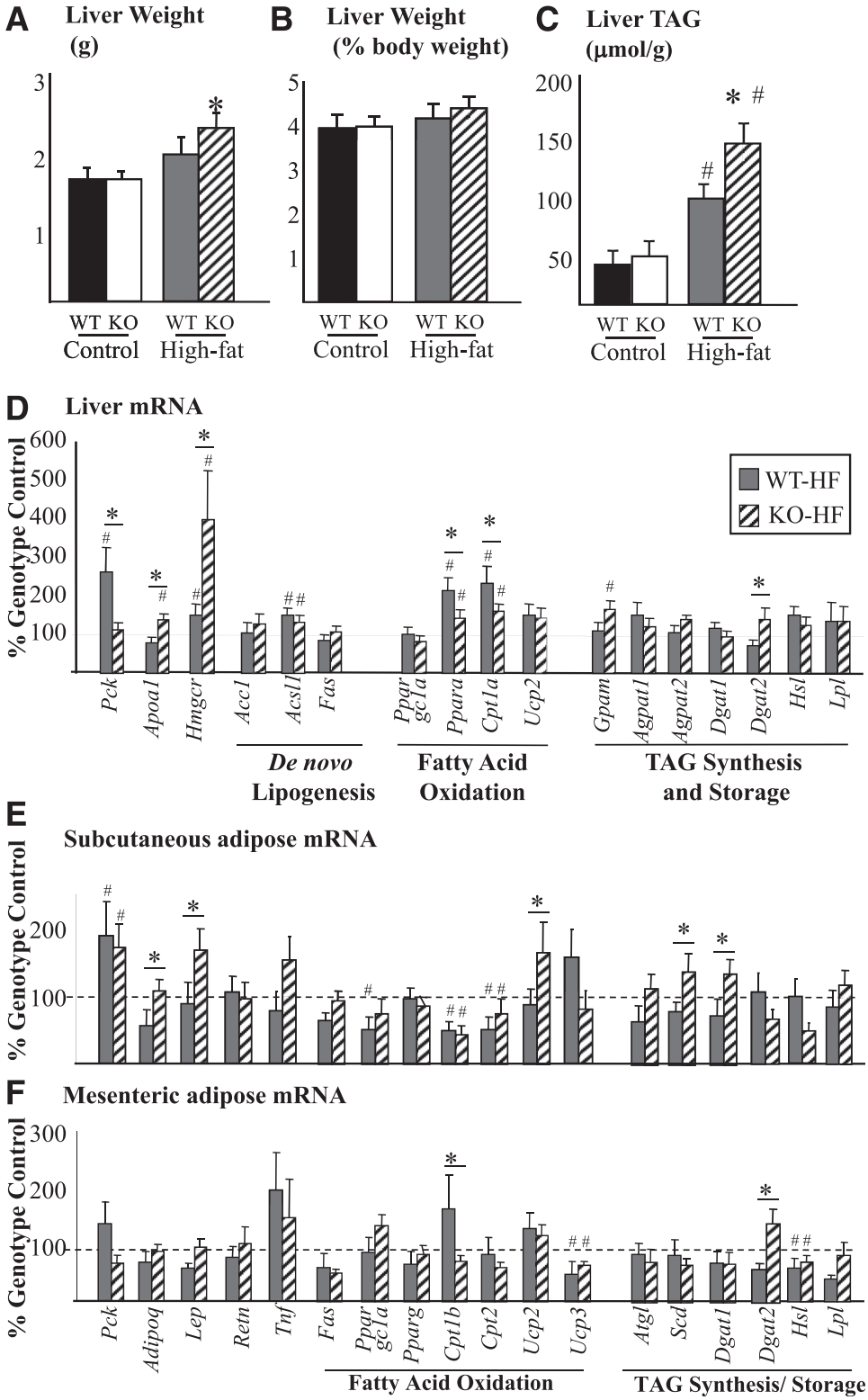

Figure 3—Hepatic fuel metabolism in male 5αR1-KO and WT mice. 5αR1-KO mice gained more liver weight (*A*) on a high-fat (HF) diet than their littermate controls (WT), although there were no differences in liver weight when presented as a percentage of body weight (*B*). *C*: Higher absolute liver weight was accompanied by increased hepatic triglyceride (TAG) concentration. Abundance of mRNA measured by quantitative real-time PCR and corrected for the mean of the abundances of three reference genes (*Rn18s*, *Ppia*, and *Tbp*) in liver (*D*), subcutaneous adipose tissue (*E*), and mesenteric adipose tissue (*F*). Changes induced by high-fat diet are shown expressed as a percentage of their genotype control. Black bars denote WT mice, and open bars denote KO mice being fed a control diet; gray bars denote WT mice, and striped bars denote KO mice being fed a high-fat diet. Data are the mean ± SEM, compared by ANOVA followed by post hoc testing with Fisher least significant differences test if appropriate. **P* < 0.05 for difference between genotypes within diet; #*P* < 0.05 for effect of diet within genotype. *n* = 7–9/group. Gene names and associated proteins are detailed in Supplementary Table 1.

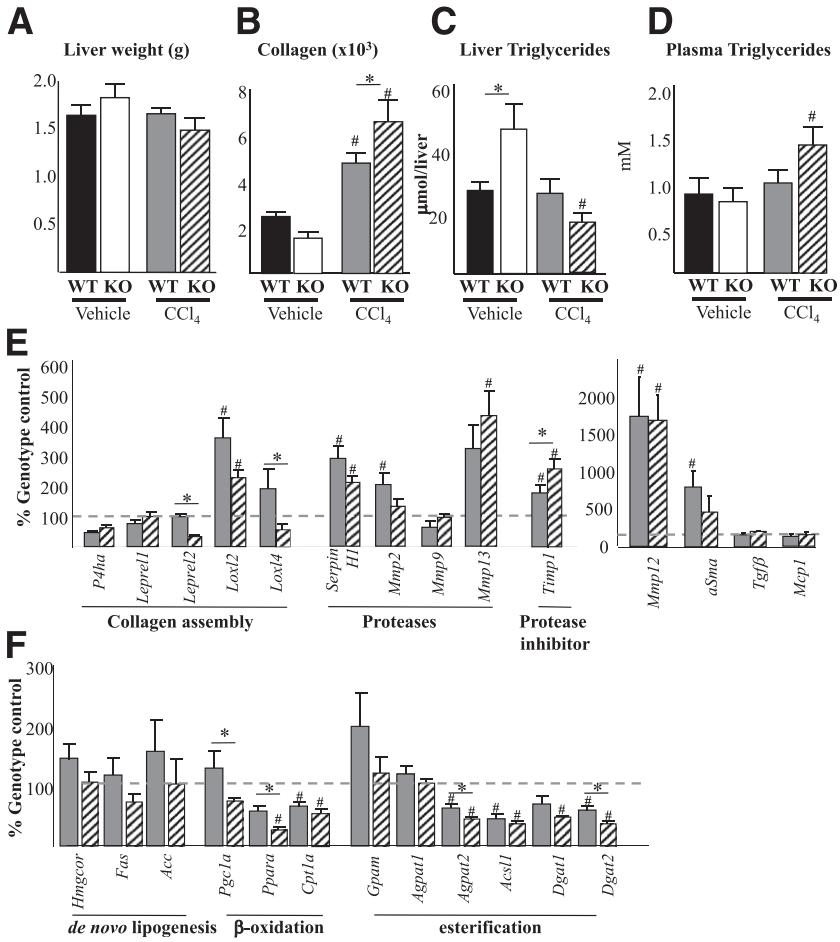

Figure 4—Response to liver injury in 5αR1-KO and WT mice. Liver weight (*A*) was not altered by CCl_4 administration, but collagen (*B*) (assessed by pixel counting after staining with picrosirius red) was increased to a greater extent in 5αR1-KO mice vs. WT controls. *C* and *D*: KO mice receiving vehicle injections had higher liver fat levels than WT mice, but this was depleted after fibrotic challenge, accompanied by increased levels of circulating triglycerides. Transcript levels reflecting liver injury response (*E*), stellate cell activation (*F*), and metabolism (*G*) show KO mice had higher levels of *Timp*1 transcript in the liver, without evidence of differential stellate cell activation. *Agpat2* and *Dgat2* were suppressed to a greater extent in KO mice than WT mice, supporting the export of liver triglycerides. Black bars denote WT mice, and open bars denote KO mice being fed vehicle treatment; gray bars denote WT mice, and striped bars denote KO mice after treatment with CCl_4. Data are the mean ± SEM, compared by ANOVA followed by post hoc testing by Fisher least significant differences test if appropriate. #$P < 0.05$ for effect of CCl_4 within genotype; *$P < 0.05$ for difference between genotypes within treatment. n = 4–8/group. Gene names and associated proteins are detailed in Supplementary Table 1.

β-oxidation (*Pgc1α* and *Pparα*) and esterification (*Agpat2* and *Dgat2*).

Pharmacological Inhibition of 5αRs in Rats Mimics the Phenotype of 5αR1 Deficiency in Mice

Finasteride was used to inhibit both 5αR1 and 5αR2 in male Zucker rats, since it is nonselective for isozymes in rats (21,25), achieving circulating concentrations of 14.2 ± 0.67 ng/mL in treated animals, and is within the therapeutic window in humans (20). A pharmacodynamic effect was confirmed by a marked decrease in prostate weight compared with vehicle (vehicle 174.0 ± 6.7 vs. finasteride 116.6 ± 7.1 mg, $P < 0.01$). Short-term treatment with finasteride did not increase weight gain or liver weight in obese rats (Fig. 6*A* and *B*). However, finasteride increased the area under the curve (AUC) for plasma glucose and insulin during a GTT (Fig. 6*C–F*), and increased hepatic triglyceride content in obese animals (Fig. 6*H*), although plasma triglycerides were unaffected (Fig. 6*G*). The liver transcript profile of selected genes, known to change in 5αR1-KO mice being fed a high-fat diet was explored. Inhibition of 5αRs again suppressed the abundance of *Cpt1a* and *Pparγ* mRNA (Fig. 6*I*), along with *Pepck*. However, in this short-term model, the down-regulation of transcripts regulating fatty acid synthesis was also observed.

To assess the dependence of the phenotype on androgens, further male obese Zucker rats were treated with finasteride or vehicle after gonadectomy or sham surgery. Again, finasteride treatment reduced prostate weight in obese rats (Table 2), but prostates in gonadectomized (GDX) rats were too shrunken to recover. Lack of testosterone in plasma confirmed successful gonadectomy (Table 2). In sham-operated animals, but not in

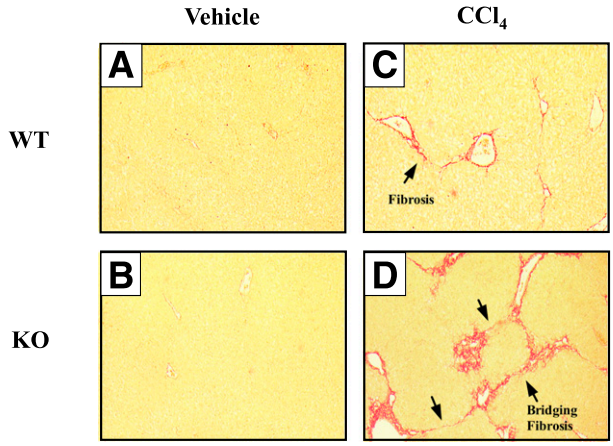

Figure 5—Liver fibrosis after CCl_4 injury in 5αR1-KO and WT mice. Representative images of liver sections (5 μm) stained with picrosirius red to show collagen deposition. Collagen is not detected in WT mice (*A*) or KO mice (*B*) receiving injections of vehicle. Mice deficient in 5αR1 have greater induction of collagen after CCl_4 administration, including evidence of bridging fibrosis (KO) (*D*), compared with WT controls (*C*).

GDX animals, finasteride increased weight gain although finasteride increased liver triglycerides to a similar degree, irrespective of prior gonadectomy (Table 2). Finasteride did not alter glucose or insulin homeostasis in sham-operated rats, but gonadectomy increased fasting glucose levels, and the combination of GDX with finasteride decreased fasting insulin levels. There was no effect of finasteride on the AUC for either glucose or insulin in sham-operated or GDX rats, or on plasma lipid profiles (Table 2).

DISCUSSION

These data demonstrate that the enzyme 5αR1 influences predisposition to metabolic disease, affecting not only a predisposition to hepatic steatosis but also influencing body fat distribution and insulin sensitivity. Moreover, increased susceptibility to steatosis was accompanied by enhanced susceptibility to fibrotic liver injury, suggesting that 5αR deficiency or inhibition may be associated with accelerated progression of nonalcoholic fatty liver disease. Similar observations with pharmacological inhibition of 5αRs in rats emphasize the potential importance of these observations in men treated with 5αR inhibitors (20).

Glucocorticoid excess in metabolic tissues is a known risk factor for insulin resistance and features of the metabolic syndrome, including obesity. This has been elegantly demonstrated by adverse metabolic phenotypes in mice overexpressing the glucocorticoid-regenerating enzyme 11β-hydroxysteroid dehydrogenase type 1 in liver (29) and adipose tissue (30). Our findings that 5αR1-KO mice eating a high-fat diet are predisposed to steatosis and insulin resistance were replicated in rats treated with a 5αR inhibitor, and align with recent findings of adverse changes in insulin sensitivity and adiposity in men receiving treatment with dual 5αR inhibitors for 3 months (20). Zucker rats were chosen for this study since pharmacological inhibitors of murine 5αR1 have not been characterized, and Zucker rats are a known model of glucocorticoid-sensitive obesity and insulin resistance (31). Finasteride is a nonselective inhibitor in rats, inhibiting both 5αRs (21,25), and many of the adverse features observed in mice were recapitulated even after only 3 weeks of finasteride treatment, with steatosis being a highly robust finding. Insulin resistance, which is associated with steatosis, was observed after finasteride treatment in unmanipulated rats, but not after sham surgery; this may relate to the short duration of finasteride treatment in rats, at just 3 weeks, and the altered stress responses after 5αR1 inhibition in the postoperative period (11). The converse was true for drug-induced weight gain, which was revealed in the sham-operated animals receiving finasteride.

Importantly, the development of steatosis in rats was detected in all animals treated with finasteride and appeared to be independent of androgen synthesis, persisting in castrated male rats. Others have reported recently that the 5αR1-KO mice are more susceptible to hepatocellular carcinoma after prolonged feeding (12 months) on the American lifestyle–induced obesity syndrome (ALIOS) diet (19), and that liver transcript changes in 5αR1-KO mice overlap with those induced by the administration of glucocorticoids rather than androgens (19). Given that we have demonstrated impaired hepatic metabolic clearance of corticosterone in 5αR1-KO mice (11) and persistence of the effect of finasteride in GDX rats, we conclude that local glucocorticoid excess is the most likely mechanism underpinning hepatic steatosis in 5αR1 deficiency or inhibition; combined alterations in androgen and/or glucocorticoid signaling may contribute to other aspects of the adverse metabolic phenotype.

The liver is the most abundant site of 5αR1 expression in rodent species (5) and the likely major target organ for the metabolic effects of 5αR1 deficiency. The abundance of 5αR1 remains unchanged in WT mice after being fed a high-fat diet, similar to that in Wistar rats (32). With high-fat feeding, differences in transcriptional responses in livers of 5αR1-KO mice were consistent with the shunting of fatty acids away from β-oxidation (lack of induction of *Cpt1a* and its key transcription factor *Pparα*) and from export as VLDL, in favor of triglyceride synthesis and cytosolic storage (selective upregulation of *mGpat* [33] and *Dgat2* [34]); glucocorticoids are known to increase the expression of *Dgat2* in hepatocytes (35). In Zucker obese rats, *Dgat2* was downregulated by finasteride, perhaps reflecting differential control of this leptin-regulated transcript (36) in these leptin-resistant rats. This suggests that leptin is not a key player in the metabolic consequences of the loss of 5αR1, which are maintained in both mice and Zucker rats. Liver transcript and circulating levels of apoA1 (the major lipoprotein in HDL), which is inducible by glucocorticoids (37), were higher after high-fat feeding

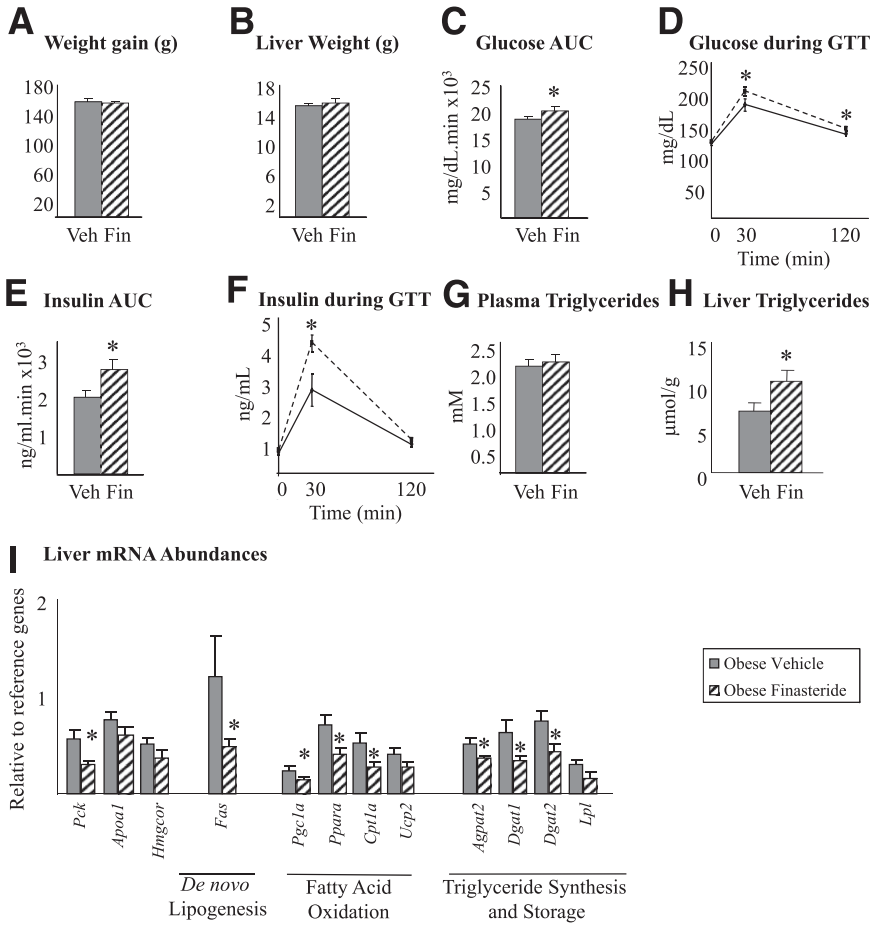

Figure 6—Effect of dual 5αR inhibition on metabolic abnormalities in male obese Zucker rats. Weight gain during the 3-week treatment period (*A*) and liver weight measured in fresh tissue (*B*) were not altered by finasteride (Fin) compared with vehicle (Veh) treatment. The AUC for glucose (*C*) and insulin (*E*) for the 90-min duration of the oral GTT were increased after finasteride treatment. Glucose was higher at 30 and 90 min (*D*), and insulin was higher at 30 min (*F*) after glucose administration in obese rats treated with finasteride (dotted line) compared with vehicle (solid line). Plasma triglyceride levels (*G*) were unaffected, and hepatic triglyceride levels (*H*) were increased by finasteride. Abundance of mRNA in liver, measured by quantitative real-time PCR and corrected for the mean of the abundance of reference genes (*Rn18s* and *Ppia*) (*I*). Gray bars are control obese rats, and striped bars are obese rats that received finasteride treatment. Data are the mean ± SEM, compared by Student *t* test. **P* < 0.05, *n* = 8–9/group. Gene names and associated proteins are detailed in Supplementary Table 1.

in 5αR1-deficient mice, and followed a similar pattern in obese rats with pharmacological inhibition of 5αRs. The lack of upregulation of the classically glucocorticoid-regulated transcript *Pepck* in livers of 5αR1-deficient mice may reflect samples having been obtained after ad libitum feeding, since PEPCK is regulated in an opposing and coordinated manner by glucocorticoids and insulin (38). Importantly, these transcript profile changes with 5αR1 deficiency do not support increased lipogenesis, contrasting with the hepatic androgen receptor KO mouse (39), emphasizing that our findings are inconsistent with the effects of 5αR1 being mediated solely through local androgen deficiency. While the disruption of 5αR1 in mice was associated with a constellation of exaggerated features of the metabolic syndrome, it is worth noting that from the age of 5 months control mice on the mixed C57BL6/SvEv/129 background were starting to increase adipose tissue and become insulin resistant; and, indeed, mice on this genetic background appear relatively resistant to metabolic challenge (19). Accordingly, some of the changes in the WT mice brought about by high-fat feeding during the period of study were modest, perhaps indicating the resistance of this strain to ad libitum high-fat feeding. In this context, the additional weight gain, liver fat, and insulin resistance in mice with 5αR1 deficiency is all the more striking.

Whether 5αR1 expression in other tissues contributes to metabolic regulation in rodents is less clear, although insulin-driven suppression of lipolysis was sustained. In the mouse, the steady-state levels of 5αR1 mRNA measured here were approximately 50-fold lower (judged by cycle number) in adipose tissue compared with liver and were not detected in skeletal muscle. There were no adverse changes in the circulating adipokine or cytokine profile in 5αR1-KO mice. 5αR1-KO mice failed to upregulate circulating leptin and resistin in response to high-fat feeding. Indeed, the lack of hyperleptinemia may underpin the exaggerated hyperphagia observed in the

Table 2—Metabolic consequences of pharmacological inhibition of 5αRs

	Sham		Gonadectomy	
	Vehicle	Finasteride	Vehicle	Finasteride
Prostate (mg)	192 ± 23	119 ± 10*	ND	ND
Testosterone (ng/mL)	0.45 ± 0.14	0.82 ± 0.25	ND	ND
Body weight at cull (g)	400 ± 21	385 ± 13	405 ± 14	378 ± 14
Weight gain (g/3 weeks)	116 ± 7.1	136 ± 6.9*	135 ± 6.3†	130 ± 6.0
Liver triglyceride (μmol/g)	33.7 ± 2.5	44.7 ± 4.8*	31.5 ± 1.6	39.8 ± 3.3*
Fasting glucose (mg/dL)	155 ± 4.0	148 ± 5.8	170 ± 4.3†	168 ± 4.5†
AUC GTT glucose (mg/dL/min $\times 10^3$)	29.8 ± 1.1	29.6 ± 1.7	31.5 ± 1.5	31.9 ± 1.9
Fasting insulin (ng/mL)	11.6 ± 1.8	12.5 ± 2.1	9.8 ± 2.0	7.00 ± 0.8†
AUC GTT insulin (ng/mL/min × 10^3)	3.3 ± 0.50	3.2 ± 0.49	2.9 ± 0.48	2.6 ± 0.32
Fasting cholesterol (mmol/L)	2.6 ± 0.26	2.4 ± 0.20	2.1 ± 0.21	2.1 ± 0.15
Fasting triglycerides (mmol/L)	2.0 ± 0.22	1.9 ± 0.22	1.5 ± 0.19	1.6 ± 0.2
Fasting NEFAs (mmol/L)	1.9 ± 0.19	2.0 ± 0.08	1.9 ± 0.09	1.9 ± 0.11

Data are the mean ± SEM, compared by two-way ANOVA and Fisher post hoc tests. ND, not detected/recovered. *$P < 0.05$ for effect of finasteride within either sham-operated or GDX rats. †$P < 0.05$ for effect of gonadectomy within either vehicle- or finasteride-treated rats.

5αR1-KO mice. However, changes were observed in mesenteric adipose transcripts, suggesting the impaired stimulation of transport by *Cpt1b* of fatty acids for oxidation in response to high-fat feeding; correspondingly, *Dgat2* mRNA (involved in triglyceride storage) was upregulated. In subcutaneous adipose tissue, the transcript profile of 5αR1-deficient mice again suggested compensatory changes to ameliorate against obesity with increased expression of *Scd* (40), *Ucp2*, and *Dgat 1* mRNA. The leptin transcript was more abundant, which is in keeping with weight gain, although circulating levels were unaltered. These changes in adipose tissue may be indirect, mediated by altered prevailing insulin concentrations, or direct, mediated by altered local steroid signaling. Androgen deficiency in fat, exemplified in adipose-specific androgen receptor knockdown in mice (41), is characterized by increased obesity and insulin resistance, but is accompanied by increases in transcripts for *Fas*, *Atgl*, *Lpl*, and *Hsl*. These changes were not observed in 5αR1-KO mice, again supporting a role for glucocorticoids rather than androgens in their phenotype.

Hepatic steatosis is a risk factor for the progression of fatty liver disease toward fibrotic changes, but the mechanisms determining this progression are not fully understood. Not all models of hepatic steatosis are predisposed to fibrosis, with exceptions including leptin-deficient mice (42), but the influence of steroid signaling on the progression of nonalcoholic fatty liver disease is unknown. We found that 5αR1-KO mice were more susceptible to developing irreversible fibrosis, with bridging changes, in response to CCl_4. Fibrosis in the CCl_4 model was accompanied by rapid depletion of the excess hepatic triglycerides, with the extra lipid load possibly spilling into plasma, although the temporal dynamics of this relationship are difficult to dissect. Export of triglycerides from the liver was supported by the suppression of *Dgat2* and *Agpat2*. However, the drive to accumulate lipid was still evident in the transcriptional profile, with downregulation of *Pparα* and its regulator *Pgc1α* typical of less oxidation and increased fatty acid synthase. Markers of hepatic stellate cell activation increased to the same extent in WT and 5αR1-KO mice, similar to the findings of Dowman et al. (19). The development of liver fibrosis represents a balance between matrix deposition and collagen synthesis and resorption. The clearance of extracellular matrix may be less effective in 5αR1-KO mice, since *Timp*1 was not induced to the same extent as in WT mice. Some enzymes involved with collagen cross-linking were suppressed in 5αR1-KO mice, which may have influence on protein stability and solubility. These data are complementary to those of Dowman et al. (19), who found that in mice fed an ALIOS diet hepatic triglycerides accumulated over a 6-month period, but that at a later stage, when fibrosis had developed, the excess lipid was depleted, although we did not assess liver histology in 5αR1-KO mice being fed a high-fat diet.

A recently published study (19) documented a similar susceptibility to hepatic steatosis in 5αR1-KO mice being fed an ALIOS diet, but showed no changes in body fat distribution or insulin sensitivity and no difference in liver fibrosis. It is likely that our experiments induced a greater metabolic challenge, with a higher fat content in the diet, and a greater degree of liver injury induced by CCl_4. However, the previous study reported only glucose measurements made during GTT and found no differences between genotypes in fasting glucose levels or AUC. Here, we also show normal glucose levels but demonstrate that the insulin response to glucose challenge is increased, which is consistent with insulin resistance. Interestingly, the previous study showed that, despite having steatosis, 5αR1-KO mice on the ALIOS diet were protected against

hepatocellular carcinoma, a further downstream pathology, although carcinoma was not evident in any of the groups studied here.

There are several potentially clinically important implications of these findings. Upregulation of 5α-reduction of steroids in metabolic disease (12,15) might serve as a protective response, lowering intracellular glucocorticoid levels. Conversely, downregulation observed in critical illness (18) may increase susceptibility to liver injury. In a population-based study (43), men with fatty livers had reduced relative excretion of 5α-reduced cortisol metabolites, which may be an important factor in their liver fat accumulation. Moreover, the abundance of 5αR1 protein in human liver correlates with features of steatohepatitis (19). Although not as widely prescribed as finasteride, which is selective for 5αR2 in humans, the nonselective "dual" inhibitor dutasteride may be prescribed more commonly, particularly for the treatment of prostate cancer, to maximally suppress dihydrotestosterone levels and hence to restrain tumor growth or recurrence (44). These data in mice suggest that understanding the effects of dutasteride on insulin sensitivity and fat distribution in adipose tissue and liver is a high priority for further studies, and this assertion is corroborated by the recent demonstration in humans of adverse metabolic changes after short-term 3-month treatment with dutasteride, although without any evidence of changes in circulating levels of markers of liver inflammation (20). In humans receiving a dual 5αR inhibitor, adverse changes in insulin resistance may be mediated by impaired glucose disposal, mainly in muscle where 5αR1 is expressed (20), unlike in the mouse. Concerns about possible adverse metabolic consequences of dual 5αR inhibition are particularly important given the long-term nature of treatment and the aged patient group affected, in whom risk factors for metabolic syndrome are most prevalent.

Acknowledgments. The authors thank Dr. Mala Mahendroo (University of Texas Southwestern Medical Center, Dallas, TX) for her support. The authors also thank the Wellcome Trust and British Heart Foundation for their financial support; Carolynn Cairns, Scott Denham, Karen French, Jill Harrison, Sanjay Kothiya, and Rachel McDonnell (University of Edinburgh) for excellent technical support; the staff of the Genetic Screening and Intervention Technologies, University of Edinburgh, for rederivation services; the Histology Shared University Research Facilities, University of Edinburgh, for histology services; and the Wellcome Trust Clinical Research Facility Mass Spectrometry Core Laboratory (University of Edinburgh) for analytical support.

Funding. This research was supported by Wellcome Trust grant 072217/Z/03/Z and British Heart Foundation grants FS/08/063 and FS/08/065.

Duality of Interest. No potential conflicts of interest relevant to this article were reported.

Author Contributions. D.E.W.L. helped to design the study, perform the experiments, and write the manuscript. P.B. helped to perform the experiments and revise the manuscript. E.M.D.R., G.A.R., B.A.W., and E.A.R.-Z. helped to perform the experiments. D.P.M. and B.R.W. helped to design the study and revise the manuscript. R.A. helped to design the study and write the manuscript. R.A. is the guarantor of this work and, as such, had full access to all the data in the study and takes responsibility for the integrity of the data and the accuracy of the data analysis.

Prior Presentation. Parts of this study were presented in abstract form at ENDO 2008: The Endocrine Society 90th Annual Meeting, San Francisco, CA, 15–18 June 2008, and the Society for Endocrinology BES 2013, Harrogate, U.K., 18–21 March 2013.

References

1. Jones MEE, Thorburn AW, Britt KL, et al. Aromatase-deficient (ArKO) mice have a phenotype of increased adiposity. Proc Natl Acad Sci U S A 2000;97:12735–12740
2. Kotelevtsev Y, Holmes MC, Burchell A, et al. 11beta-hydroxysteroid dehydrogenase type 1 knockout mice show attenuated glucocorticoid-inducible responses and resist hyperglycemia on obesity or stress. Proc Natl Acad Sci U S A 1997;94:14924–14929
3. Morton NM, Holmes MC, Fiévet C, et al. Improved lipid and lipoprotein profile, hepatic insulin sensitivity, and glucose tolerance in 11β-hydroxysteroid dehydrogenase type 1 null mice. J Biol Chem 2001;276:41293–41300
4. Russell DW, Wilson JD. Steroid 5 α-reductase: two genes/two enzymes. Annu Rev Biochem 1994;63:25–61
5. Thigpen AE, Silver RI, Guileyardo JM, Casey ML, McConnell JD, Russell DW. Tissue distribution and ontogeny of steroid 5 α-reductase isozyme expression. J Clin Invest 1993;92:903–910
6. Barat P, Livingstone DEW, Elferink CM, McDonnell CR, Walker BR, Andrew R. Effects of gonadectomy on glucocorticoid metabolism in obese Zucker rats. Endocrinology 2007;148:4836–4843
7. Wake DJ, Strand M, Rask E, et al. Intra-adipose sex steroid metabolism and body fat distribution in idiopathic human obesity. Clin Endocrinol (Oxf) 2007;66:440–446
8. Aizawa K, Iemitsu M, Maeda S, et al. Acute exercise activates local bioactive androgen metabolism in skeletal muscle. Steroids 2010;75:219–223
9. Normington K, Russell DW. Tissue distribution and kinetic characteristics of rat steroid 5 α-reductase isozymes. Evidence for distinct physiological functions. J Biol Chem 1992;267:19548–19554
10. Gisleskog PO, Hermann D, Hammarlund-Udenaes M, Karlsson MO. A model for the turnover of dihydrotestosterone in the presence of the irreversible 5α-reductase inhibitors GI98745 and finasteride. Clin Pharmacol Ther 1998;64:636–647
11. Livingstone DEW, Di Rollo EM, Yang C, et al. Relative adrenal insufficiency in mice deficient in 5a-reductase 1. J Endocrinol 2014;222:257–266
12. Andrew R, Phillips DIW, Walker BR. Obesity and gender influence cortisol secretion and metabolism in man. J Clin Endocrinol Metab 1998;83:1806–1809
13. Ahmed A, Rabbitt E, Brady T, et al. A switch in hepatic cortisol metabolism across the spectrum of non alcoholic fatty liver disease. PLoS One 2012;7:e29531
14. Fassnacht M, Schlenz N, Schneider SB, Wudy SA, Allolio B, Arlt W. Beyond adrenal and ovarian androgen generation: increased peripheral 5 α-reductase activity in women with polycystic ovary syndrome. J Clin Endocrinol Metab 2003;88:2760–2766
15. Fraser R, Ingram MC, Anderson NH, Morrison C, Davies E, Connell JMC. Cortisol effects on body mass, blood pressure, and cholesterol in the general population. Hypertension 1999;33:1364–1368
16. Stewart PM, Shackleton CHL, Beastall GH, Edwards CRW. 5 alpha-reductase activity in polycystic ovary syndrome. Lancet 1990;335:431–433
17. Tsilchorozidou T, Honour JW, Conway GS. Altered cortisol metabolism in polycystic ovary syndrome: insulin enhances 5α-reduction but not the elevated adrenal steroid production rates. J Clin Endocrinol Metab 2003;88:5907–5913
18. Boonen E, Vervenne H, Meersseman P, et al. Reduced cortisol metabolism during critical illness. N Engl J Med 2013;368:1477–1488
19. Dowman JK, Hopkins LJ, Reynolds GM, et al. Loss of 5α-reductase type 1 accelerates the development of hepatic steatosis but protects against hepatocellular carcinoma in male mice. Endocrinology 2013;154:4536–4547
20. Upreti R, Hughes KA, Livingstone DE, et al. 5α-reductase type 1 modulates insulin sensitivity in men. J Clin Endocrinol Metab 2014;99:E1397–E1406
21. Thigpen AE, Russell DW. Four-amino acid segment in steroid 5 α-reductase 1 confers sensitivity to finasteride, a competitive inhibitor. J Biol Chem 1992;267:8577–8583

22. Mahendroo MS, Cala KM, Russell DW. 5 α-reduced androgens play a key role in murine parturition. Mol Endocrinol 1996;10:380–392
23. Mahendroo MS, Cala KM, Landrum DP, Russell DW. Fetal death in mice lacking 5alpha-reductase type 1 caused by estrogen excess. Mol Endocrinol 1997;11:917–927
24. Constandinou C, Henderson N, Iredale JP. Modeling liver fibrosis in rodents. Methods Mol Med 2005;117:237–250
25. Azzolina B, Ellsworth K, Andersson S, Geissler W, Bull HG, Harris GS. Inhibition of rat alpha-reductases by finasteride: evidence for isozyme differences in the mechanism of inhibition. J Steroid Biochem Mol Biol 1997; 61:55–64
26. Livingstone DEW, Walker BR. Is 11β-hydroxysteroid dehydrogenase type 1 a therapeutic target? Effects of carbenoxolone in lean and obese Zucker rats. J Pharmacol Exp Ther 2003;305:167–172
27. Holmes MC, French KL, Seckl JR. Modulation of serotonin and corticosteroid receptor gene expression in the rat hippocampus with circadian rhythm and stress. Brain Res Mol Brain Res 1995;28:186–192
28. Raubenheimer PJ, Nyirenda MJ, Walker BR. A choline-deficient diet exacerbates fatty liver but attenuates insulin resistance and glucose intolerance in mice fed a high-fat diet. Diabetes 2006;55:2015–2020
29. Paterson JM, Morton NM, Fievet C, et al. Metabolic syndrome without obesity: hepatic overexpression of 11β-hydroxysteroid dehydrogenase type 1 in transgenic mice. Proc Natl Acad Sci U S A 2004;101:7088–7093
30. Masuzaki H, Paterson J, Shinyama H, et al. A transgenic model of visceral obesity and the metabolic syndrome. Science 2001;294:2166–2170
31. Livingstone DE, Kenyon CJ, Walker BR. Mechanisms of dysregulation of 11 beta-hydroxysteroid dehydrogenase type 1 in obese Zucker rats. J Endocrinol 2000;167:533–539
32. Drake AJ, Livingstone DEW, Andrew R, Seckl JR, Morton NM, Walker BR. Reduced adipose glucocorticoid reactivation and increased hepatic glucocorticoid clearance as an early adaptation to high-fat feeding in Wistar rats. Endocrinology 2005;146:913–919
33. Lewin TM, Wang S, Nagle CA, Van Horn CG, Coleman RA. Mitochondrial glycerol-3-phosphate acyltransferase-1 directs the metabolic fate of exogenous fatty acids in hepatocytes. Am J Physiol Endocrinol Metab 2005;288:E835–E844
34. Yamazaki T, Sasaki E, Kakinuma C, Yano T, Miura S, Ezaki O. Increased very low density lipoprotein secretion and gonadal fat mass in mice overexpressing liver DGAT1. J Biol Chem 2005;280:21506–21514
35. Dolinsky VW, Douglas DN, Lehner R, Vance DE. Regulation of the enzymes of hepatic microsomal triacylglycerol lipolysis and re-esterification by the glucocorticoid dexamethasone. Biochem J 2004;378:967–974
36. Suzuki R, Tobe K, Aoyama M, et al. Expression of DGAT2 in white adipose tissue is regulated by central leptin action. J Biol Chem 2005;280:3331–3337
37. Hargrove GM, Junco A, Wong NCW. Hormonal regulation of apolipoprotein AI. J Mol Endocrinol 1999;22:103–111
38. Hanson RW, Reshef L. Regulation of phosphoenolpyruvate carboxykinase (GTP) gene expression. Annu Rev Biochem 1997;66:581–611
39. Lin H-Y, Yu I-C, Wang R-S, et al. Increased hepatic steatosis and insulin resistance in mice lacking hepatic androgen receptor. Hepatology 2008;47:1924–1935
40. Cohen P, Ntambi JM, Friedman JM. Stearoyl-CoA desaturase-1 and the metabolic syndrome. Curr Drug Targets Immune Endocr Metabol Disord 2003;3: 271–280
41. McInnes KJ, Smith LB, Hunger NI, Saunders PTK, Andrew R, Walker BR. Deletion of the androgen receptor in adipose tissue in male mice elevates retinol binding protein 4 and reveals independent effects on visceral fat mass and on glucose homeostasis. Diabetes 2012;61:1072–1081
42. Leclercq IA, Farrell GC, Schriemer R, Robertson GR. Leptin is essential for the hepatic fibrogenic response to chronic liver injury. J Hepatol 2002;37:206–213
43. Westerbacka J, Yki-Järvinen H, Vehkavaara S, et al. Body fat distribution and cortisol metabolism in healthy men: enhanced 5β-reductase and lower cortisol/cortisone metabolite ratios in men with fatty liver. J Clin Endocrinol Metab 2003;88:4924–4931
44. Mohler JL, Titus MA, Wilson EM. Potential prostate cancer drug target: bioactivation of androstanediol by conversion to dihydrotestosterone. Clin Cancer Res 2011;17:5844–5849